



# Variations of Solar Radius: Observations with RHESSEI

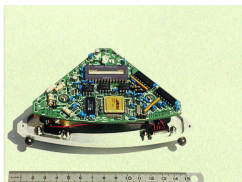
M.D. Fivian, H.S. Hudson, R.P. Lin, Space Sciences Laboratory, UC-Berkeley

Email: mfivian@ssl.berkeley.edu

The Solar Aspect System (SAS) of the rotating (at 15 rpm) RHESSEI spacecraft has three subsystems. Each of these measures the position of the limb by sampling the full solar chord profile with a linear CCD using a narrow-band filter at 670 nm. With a CCD pixel size of 1.7 arcsec, the accuracy of each of the 6 limb positions is theoretically better than 50 mas using 4 pixels at each limb. Since the launch of RHESSEI early 2002, solar limbs have been sampled with at least 100 Hz. The database currently exceeds  $4 \times 10^9$  individual radius measurements. The main function of SAS is to determine the RHESSEI pointing relative to Sun center. The observed precision of this determination has a typical instantaneous (16 Hz) value of the order of 50 mas (rms). As a byproduct of this we observe the solar oblateness and see signatures of magnetic activity (spots and faculae). We present these first RHESSEI results here.

## The SAS Instrument

- Design: 3 independent subsystems on rotating S/C
- Optics: f/40 coated lens, 670 nm (12 nm FWHM) bandpass filter, 1550 mm focal length
- Sensor: three linear CCDs with 2048 pixels, length: 13  $\mu\text{m}/\text{pixel}$ , total 26mm width: 13  $\mu\text{m}/\text{pixel}$ , integration: programmable, typical 700  $\mu\text{sec}$  resolution: 10 bit @ 128 Hz
- Sun Image: 14.4 mm
- Field of View: single CCD: 59 arcmin, high resolution: 27 arcmin
- Resolution: 1.73 arcsec/pixel, 0.133 arcsec/ $\mu\text{m}$



Geometry of SAS with real and mis-calculated sun center

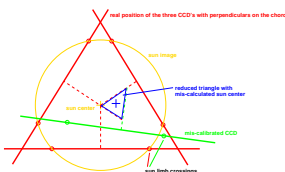
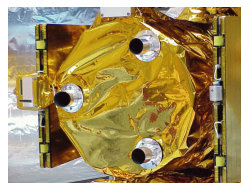


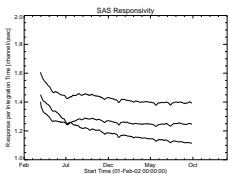
Image of one of the three SAS sensors with the front-end electronics. The cover with the integrated blocking filter is not shown.



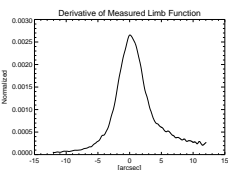
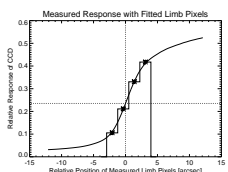
The image of the sunny side of the integrated spacecraft shows the three baffles for the SAS lenses which are coated with a bandpass filter.

The drawing on the left shows a sketch of the SAS geometry. The three lenses focus the solar disc at 670 nm onto the three linear CCDs. Knowing the effective geometry and relating the three subsystems correctly leads to the indicated reconstruction of the sun center. Any deviation from the correct geometry leads to an ambiguous reconstruction and therefore a non-vanishing reduced triangle. The 9 free parameters defining the relative geometry of all SAS feature can be fitted using the enormous statistics of measured Sun limb crossings. A set of wrong parameters leads to an inconsistent reconstruction of the Sun center.

## The Calibration



Frequent readouts of the full solar profile allows a precise measurement of the responsivity.



The PSF of the three subsystems has not been measured prior to flight. Therefore it has to be estimated analysing the data. The main contribution to the width of the core is the diffraction at the lens and chromatic aberration. The estimated value prior to flight is 4.3 arcsec (FWHM). Averaging over several 10'000 of profile measurements results in a well sampled limb profile function. This measured limb profile contains the physical solar limb darkening at 670 nm convoluted with the instrumental response.

In first order, the solar profile at 670 nm can be approximated with a step function. Therefore, the derivative of the measured and normalized limb profile gives a rough estimate of the core of the PSF. The measured width of 4.5 arcsec (FWHM) confirms the integrated measured profile.

In order to measure the side lobes of the PSF, the measured profiles have to be de-convoluted using a model for the limb darkening function.

The responsivity for each of the three SAS subsystems is measured in channels per  $\mu\text{sec}$ . The overall decrease of responsivity is caused by degrading of the lenses. Whereas two of the three subsystems are stabilized over time, one lens still continues to degrade. This remaining degrading doesn't compromise the data since the integration time can be adjusted in order to use the full resolution of the data.

The smaller changes in responsivity, on the time scale of weeks, is correlated with the varying duration of exposure to sun light and a subsequent small variation of the temperature of the sensor.

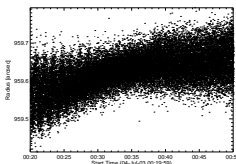
For every integration time, the four triggered pixels at each of the measured solar limb are fitted to the corresponding measured (averaged) limb profile function. The statistics of the data shows that the determination of the solar limb has an rms error of approximately 50 mas. Therefore, for every cycle (16 Hz) 6 radii can be calculated. This forms an enormous database of relatively high precision solar radii measurements.

The measured limb profile function differs in the mission and an equivalent limb profile later in the mission. This difference suggests clearly that the limb profile flattens over time, which means that the width of the PSF increases in time. Wiggles (e.g. at 10 arcsec) indicate information about the side lobes of the PSF.

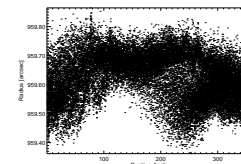
The upper plot shows the difference between an averaged limb profile for a time range early in the mission and an equivalent limb profile later in the mission. This difference suggests clearly that the limb profile flattens over time, which means that the width of the PSF increases in time. Wiggles (e.g. at 10 arcsec) indicate information about the side lobes of the PSF.

The lower plot shows the difference between averaged limb profiles at two opposite off-axis angles for one subsystem. The measured limb profile, and therefore the PSF, depends significantly on the off-axis angle. Therefore, coma effects of the lens can and have to be quantified.

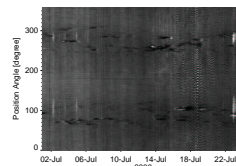
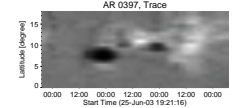
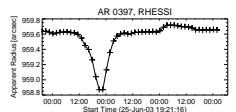
## Status of Data Analysis



Individual points plotted as a function of time for the same orbit. This gives a feeling for the large number of measures available, and the distribution of points indicates the presence of systematic error terms that are not fully corrected yet.

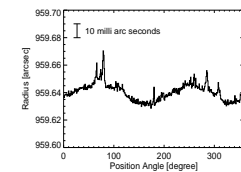


Individual radius measurements plotted as a function of the heliographic position angle. The rich structure seems to carry information about discrepancies in the calibration.



Synoptic view of limb shape data for the first half of July, 2003, with solar position angle 180 degree (South) at the middle. The image is negative (faculae appear dark) and covers a range of about 2 arcsec effective radius. The faculae and sunspots appear in the active latitudes and are brightness changes here rather than radius variations.

East limb passage of NOAA active region 0397, observed at 2003 June 26, 0:30 UT. The map (bottom) shows limb latitudes from the equator to N20, and the line plot (top) corresponds to N08. The time resolution of the data is one RHESSEI orbit, or 96 min. The data essentially show excess brightness as apparent radius; there is plage and another smaller sunspot from AR 0399 following the appearance the larger sunspot; the two spot groups had areas of 850 and 30 millionths on July 1. In future analysis we hope to distinguish photometric effects from true radius values.



Plot showing a 50-orbit sum from the data in Figure to the left. A modulation consistent with the solar oblateness can readily be seen, along with excesses due mainly to facular brightness. There are also artifacts present as well as noise at a level of about 2 mas (RMS) in the 1 degree bins.

## Conclusion Outlook

At this point we have completed most of the work on sensor calibration and are in the process of tweaking it to suppress systematic terms of many kinds. The data shown above establish that these terms will be controllable at the level of milli-arcsec. We hope to apply these data to many purposes, especially helioseismology and the observation of solar shape variations with position and time.